

Magnetic-field induced superconductor-metal-insulator transitions in bismuth metal-graphite

Masatsugu Suzuki, Itsuko S. Suzuki, and Robert Lee

Department of Physics, State University of New York at Binghamton, Binghamton, New York 13902-6016

Jurgen Walter

Department of Materials Science and Processing, Graduated School of Engineering,
Osaka University, 2-1, Yamada-oka, Suita, 565-0879, JAPAN

(dated: March 22, 2024)

Bismuth-metal-graphite (BiMG) has a unique layered structure where Bi nanoparticles are encapsulated between adjacent sheets of nanographites. The superconductivity below T_c ($= 2.48$ K) is due to Bi nanoparticles. The Curie-like susceptibility below 30 K is due to conduction electrons localized near zigzag edges of nanographites. A magnetic-field induced transition from metallic to semiconductor-like phase is observed in the in-plane resistivity ρ_a around H_c (≈ 25 kOe) for both $H \parallel c$ and $H \parallel ab$ (c : c axis). A negative magnetoresistance in ρ_a for $H \parallel c$ ($0 < H \leq 3.5$ kOe) and a logarithmic divergence in ρ_a with decreasing temperature for $H \parallel ab$ ($H > 40$ kOe) suggest the occurrence of two-dimensional weak localization effect.

PACS numbers: 71.24.+q, 74.80.Dm, 72.15.Rn, 71.30.+h

I. INTRODUCTION

A weak localization theory predicts a logarithmic divergence of the resistivity in the two-dimensional (2D) electron systems as the temperature (T) is lowered.¹ In high-mobility Si metal oxide-semiconductor field-effect transistor (MOSFET), the in-plane resistivity for a system with an electron density n larger than a critical electron density n_c decreases with decreasing T , indicating a metallic behavior.^{2,3,4} This metallic state is completely destroyed by the application of an external magnetic field (H) applied in the basal plane when H is higher than a threshold field H_c . Such coplanar fields only polarize the spins of the electrons, indicating that the spin state is significant to the high conductivity of the metallic state. The scaling relation of the in-plane resistivity collapses into two distinct branches above and below H_c . Such behaviors are very similar to those observed in amorphous ultrathin metal films of InO_x ,⁵ MoGe ,^{6,7} and Bi ,⁸ which undergo magnetic field-induced transitions from superconducting phase to insulating phase.

Bi-metal-graphite (BiMG) constitutes a novel class of materials having unique layered structures. This system can be prepared from the reduction by Li-diphenylide from an acceptor-type BiCl_3 graphite intercalation compound (GIC) as a precursor material. Ideally, the staging structure of BiMG would be the same as that of BiCl_3 GIC.^{9,10,11} In BiMG, Bi atoms would form intercalate layers sandwiched between adjacent graphite layers. For the stage- n ($= 1, 2, \dots$) structure, the pack molecules and extended graphene sheets. Fujita and co-workers^{13,14,15} have theoretically suggested that the electronic structures of finite-size graphene sheets depend crucially on the shape of their edges. The graphene edge of an arbitrary shape consists of two-types of edges, zigzag type and armchair type. The former has a trans-polyacetylene type structure and the latter has a cis-polyacetylene one. Finite graphite systems having zigzag

but are unable to diffuse across the stack of layers.¹² Such a large ratio is due to the insulating BiCl_3 layer sandwiched between the adjacent graphite layers. There is no overlapping of the wave functions over nearest neighbor graphite layers. The situation may not drastically change in BiMG in spite of the fact that BiCl_3 layer is replaced by metallic Bi layer. In fact the c -axis resistivity of BiMG (≈ 0.1 Ω cm at 298 K) is almost the same as that of BiCl_3 GIC at the same T , suggesting that BiMG behaves like a quasi-2D conductor.

In this paper we have undertaken an extensive study on the transport and magnetic properties of BiMG. We show that this compound undergoes a superconducting transition at $T_c = 2.48$ K. A magnetic-field induced transition from metallic to semiconductor-like phase is observed in ρ_a around $H_c \approx 25$ kOe for $H \parallel c$ and $H \parallel ab$ (c : c axis). These results of BiMG are compared with those of Si MOSFET, and amorphous ultrathin metal films of InO_x ,⁵ MoGe ,^{6,7} and Bi .⁸

Structural studies of BiMG reveal that Bi layers are formed of Bi nanoparticles which are encapsulated between adjacent sheets of nanographites. The size of nanographites in BiMG is much smaller than the in-plane coherence size of the graphite layers of pristine graphite. The superconductivity is mainly due to Bi nanoparticles, while the magnetism is mainly due to nanographites. Nanographites are nanometer-sized graphite fragments which represent a new class of mesoscopic system intermediate between aromatic

edges exhibit a special edge state. The corresponding energy bands are almost at the Fermi energy, thereby giving a sharp peak in the density of states (DOS) at the Fermi energy. This is in contrast to the case of 2D graphene sheet with infinite size, where the DOS is zero at the Fermi energy. According to Wakabayashi et al.,¹⁵ the magnetism of nanographites is characterized by Pauli paramagnetism and orbital diamagnetism from conduction electrons. They have predicted that the Pauli paramagnetic susceptibility for the nanographites with zigzag edges shows a Curie-like behavior at low temperatures, which is in contrast to a T -independent Pauli paramagnetism in normal metals. In this paper we show that the susceptibility of BiMG has a Curie-like behavior at low T . This behavior is discussed in the light of the prediction by Wakabayashi et al.¹⁵

II. EXPERIMENTAL PROCEDURE

BiC₃ GIC samples as a precursor material, were prepared by heating a mixture of highly oriented pyrolytic graphite (HOPG) [grade ZYA from Advanced Ceramics, Ohio] and an excess amount of BiC₃ at 200 °C in a ampoule filled with chlorine gas at a pressure of 375 Torr.^{9,10} The reaction was continued for three days. It was confirmed from (00L) x-ray diffraction (Rigaku RINT 2000 x-ray powder diffractometer) that the BiC₃ GIC sample consists of stage-2 as a majority phase and stage-3 and stage-4 as minority phase. The c axis repeat distance is 13.17 ± 0.05 Å for stage-2, 15.85 ± 0.25 Å for stage-3, and 20.22 ± 0.25 Å for stage-4, respectively. No Bragg reflection from the pristine graphite is observed.

The synthesis of BiMG was made by the reduction by Li-diphenylide from BiC₃ GIC. BiC₃ GIC samples were kept for three days in a solution of lithium diphenylide in tetrahydrofuran (THF) at room temperature. Then the samples were filtered, rinsed by THF, and dried in air. Finally the samples were annealed at 260 °C in a hydrogen gas atmosphere for one day. The structure of BiMG thus obtained was examined by (00L) x-ray diffraction, and bright field images and selected-area electron diffraction (SAED) (Hitachi H-800 transmission electron microscope) operated at 200 kV. The same methods for the structural analysis were used for Pd-MG.^{16,17,18} The (00L) x-ray diffraction pattern of BiMG is much more complicated than that of BiC₃ GIC, which makes it difficult to calculate the average particle thickness from the identity period in BiMG. Note that graphite reflections appear in BiMG, suggesting that a part of Bi atoms leaves from the graphite galleries occupied by BiC₃ intercalate layers in BiC₃ GIC during the reduction process. Such Bi atoms tend to form multilayered Binanoparticles in the graphite galleries in BiMG. The number of Bi layers in possible multilayered structures could not be exactly determined at present. SAED pattern of BiMG consists of polycrystalline diffraction rings, suggesting that there are at least four Bi layers in thickness. Re-

TABLE I: Experimentally observed spacings d_{exp} for BiMG and d_{PDF} given by powder diffraction file (PDF) 5-0519 for rhombohedral Bi [spacegroup: $R\bar{3}m$ ($a_0 = 4.546$ Å, $c_0 = 11.860$ Å for the notation of the hexagonal close-packed structure)]. All reflections can be indexed as (hkl) reflections of Bi. Graphite reflections are not included.

d_{exp} (Å)	d_{PDF} (Å)	(hkl)
3.24	3.28	102
2.35	2.39	014
1.92	1.970	113
1.71	1.868	022
1.51	1.515	025
1.40	1.443	212

fections from Bi and graphite were observed. As listed in Table I, all the Bi reflections were labeled and attributed to the formation of rhombohedral Bi, according to the standard ICDD PDF (Card No. 05-0519). This result indicates that Binanoparticles are crystallized as rhombohedral Bi phase in BiMG. The observed spacings of BiMG are 1-2 % shorter than those of bulk Bi metal. The size of Binanoparticles distribute widely around the average size 110 Å. More than 50 % of Binanoparticles has sizes ranging between 10 and 50 Å. The largest particle size is 750 Å.

The measurements of DC magnetization and resistivity were made using a SQUID magnetometer (Quantum Design MPMS XL-5) with an ultra low field capability and an external device control mode. In the present work we used a BiMG sample based on HOPG which is partially exfoliated. The stoichiometry of C and Bi was not determined. The in-plane resistivity ρ_a and the c axis resistivity ρ_c were measured by a conventional four-probe method. The sample had a rectangular form with a base 6.0×1.6 mm² and a height 0.47 mm along the c axis. For the measurement of ρ_a , four thin gold wires (25- μ m diameter) that were used as the current and voltage probes were attached to one side of the c surfaces by silver paste (4922N, du Pont). For the measurement of ρ_c , two thin gold wires as the current and voltage probes were attached to each c -surface of the sample. The current ($I = 10$ mA for ρ_a and 3 mA for ρ_c) was supplied through the current probes by a Keithley type 224, programable DC current source. The voltage V generated across the voltage probes was measured by a Keithley 182 nanovoltmeter. The linearity of I - V characteristics was confirmed for the measurements of ρ_a and ρ_c .

III. RESULT AND DISCUSSION

A. Meissner effect due to Binanoparticles

We measured the DC magnetization of BiMG. After the sample was cooled from 298 to 1.9 K at $H = 0$, the

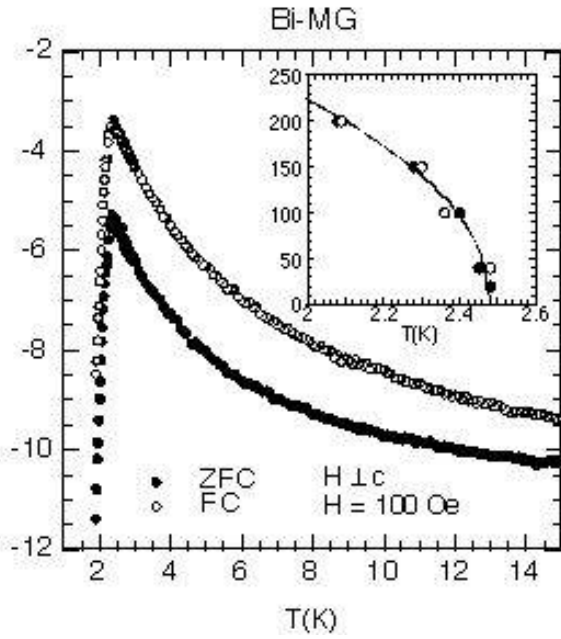


FIG. 1: T dependence of ZFC and FC susceptibilities of Bi-MG based on HOPG. $H = 100$ Oe. $H \perp c$ (c: c axis). The inset shows the magnetic phase diagram of H vs T for $H \perp c$, where the peak temperatures of ZFC and FC susceptibilities are plotted as a function of H . The solid line denotes the least-squares fit of the ZFC data (●) to Eq.(1).

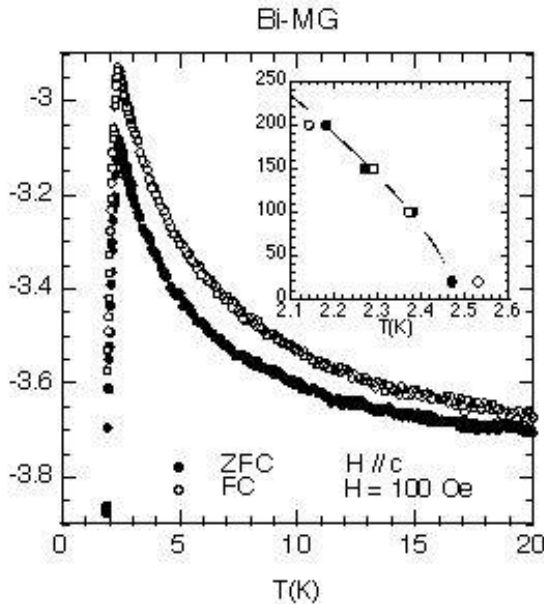


FIG. 2: T dependence of ZFC and FC susceptibilities of Bi-MG. $H = 100$ Oe. $H \parallel c$ (c: c axis). The inset shows the magnetic phase diagram of H vs T for $H \parallel c$. The solid line denotes the least-squares fitting curve for the ZFC data (●) to Eq.(1).

measurement of zero field cooled (ZFC) magnetization M_{ZFC} was made with increasing T from 1.9 to 15 K in the presence of H . The sample was kept for 20 minutes at 50 K. Then the sample was cooled from 50 to 15 K. The measurement of field-cooled (FC) magnetization M_{FC} was made with decreasing T from 15 to 1.9 K in the presence of the same H . For convenience, hereafter, the direction of H in the c plane is denoted as $H \perp c$ (c: c axis). Figures 1 and 2 show typical examples of the T dependence of the susceptibility χ_{ZFC} ($= M_{ZFC}/H$) and χ_{FC} ($= M_{FC}/H$) at $H = 100$ Oe for $H \perp c$ and $H \parallel c$, respectively. Both χ_{FC} and χ_{ZFC} show a sharp peak around 2.5 K at $H = 20$ Oe, which results from the competition between the diamagnetic susceptibility due to the Meissner effect and the Curie-like susceptibility (which will be described later). The peak shifts to the low T side with increasing H . No peak is observed above 1.9 K for $H = 250$ Oe. For convenience, the peak temperature is defined as a critical temperature $T_c(H)$. The peak temperature $T_c(H)$ for χ_{FC} is almost the same as that for χ_{ZFC} . In the insets of Figs. 1 and 2, we show the H - T magnetic phase diagram for Bi-MG for $H \perp c$ and $H \parallel c$, respectively. We find that the data of H vs T (χ_{ZFC} susceptibility) for $H \perp c$ and $H \parallel c$ are well described by

$$H = H_0 \left(\frac{T_c}{T} \right)^\beta; \quad (1)$$

where H_0 is the critical field at $T = 0$ K ($H_0 = H_{c2}$ for $H \perp c$ and $H_0 = H_{c3}$ for $H \parallel c$), β is an exponent, and T_c is a critical temperature at $H = 0$. The field H_{c3} is a field to nucleate a small superconducting region near the sample surface. The least squares fits of the data of H vs T (χ_{ZFC} susceptibility) yield the values of $H_{c2} = 489.4 \pm 0.5$ Oe, $\beta = 0.48 \pm 0.02$, $T_c = 2.48 \pm 0.06$ K for $H \perp c$, and $H_{c3} = 838 \pm 1.0$ Oe, $\beta = 0.69 \pm 0.02$, $T_c = 2.48 \pm 0.02$ K for $H \parallel c$. Here we note that the superconductivity is observed in ultrathin films of amorphous Bi grown in top of layer of amorphous Ge (thickness, 6–10 Å). Haviland et al.¹⁹ have reported that the superconductivity occurs for the thickness of Bi films, $d = 6.73 - 74.27$ Å. The critical temperature T_c decreases with decreasing d : $T_c = 5.6$ K for $d = 74.27$ Å and $T_c = 0.8$ K for $d = 6.73$ Å. Markovic et al.⁸ have shown that T_c decreases with decreasing d for $d > d_c$ ($d_c = 12.2$ Å): $T_c = 0.5$ K for $d = 15$ Å. Weitzel and Micklitz²⁰ have reported surface superconductivity in granular films built from well-defined rhombohedral Bi clusters (mean size = 38 Å) embedded in different matrices (Kr, Xe, Ge) or with H_2 or O_2 gas adsorbed on the cluster surface. The critical temperature T_c , which is dependent on matrices and gases used, is between 2 and 6 K. This value of T_c is on the same order as that of Bi-MG. The exponent β for $H \perp c$ is very close to that ($\beta = 0.5$) predicted for homogeneous system of isolated superconducting grains.²¹ The ratio H_{c3}/H_{c2} is calculated as 1.71, which is very close to the predicted value 1.695.²² Similar behavior is observed in the critical fields for $H \perp c$ and $H \parallel c$ in stage-1 K_{0.8}GIC (KCs₈).²³ The

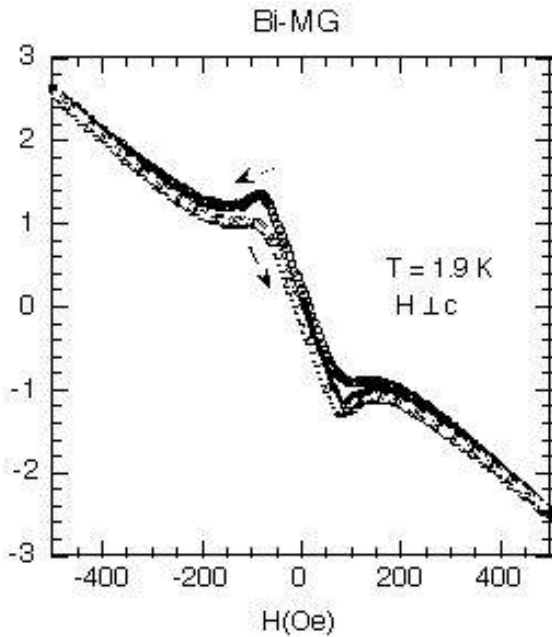


FIG. 3: Hysteresis loop of DC magnetization for Bi-MG. $H \perp c$. $T = 1.9$ K. The measurement was made with increasing H from 0 to 500 Oe (denoted by \circ), with decreasing H from 500 Oe to -500 Oe (\square), and with increasing H from -500 Oe to 500 Oe (\triangle).

coherence length is estimated as $\xi = 820$ Å from the value of H_{c2} using the relation $H_{c2} = \phi_0 / (2 \xi^2)$, where $\phi_0 (= 2.0678 \times 10^7$ Gauss cm^2) is a fluxoid. The coherence length is much larger than the size of islands (110 Å in average).

Figure 3 shows the hysteresis loop of the magnetization $M_a(H)$ for $H \perp c$ at $T = 1.9$ K. The sample was cooled from 298 K to 1.9 K at $H = 0$. The magnetization $M_a(H)$ was measured with increasing H from 0 to 500 Oe, with decreasing H from 500 Oe to -500 Oe, and with increasing H from -500 Oe to 500 Oe. The magnetization consists of superconductivity contribution and diamagnetic background. In Fig. 4(a) we show the hysteresis loop of $M_a(H)$ that is defined by $M_a(H)$ at 1.9 K minus a diamagnetic background given by $\chi_d H$ with $\chi_d = -5.143 \times 10^{-7}$ emu/gOe. A hysteresis loop characteristic to a type-II superconductor is observed with a lower critical field H_{c1} (≈ 80 Oe). In contrast, the magnetization hysteresis loop $M_a(H)$ at $T = 3.3$ K is very different from that at 1.9 K. It seems that there is neither local minimum nor local maximum. In Fig. 4(b) we show the hysteresis loop of $M_a(H)$ which is defined by $M_a(H)$ at 3.3 K minus a diamagnetic background given by $\chi_d H$ with $\chi_d = -7.317 \times 10^{-7}$ emu/gOe. As H decreases, a trapped magnetic flux, corresponding to a paramagnetic moment M_r ($\approx 2.7 \times 10^5$ emu/g) remains in the sample. With further cycling of H from -500 to 500 Oe a characteristic hysteresis loop is observed.

We also measured the hysteresis loop of the magnetization $M_c(H)$ for $H \parallel c$ at $T = 1.9$ K. The difference M_c

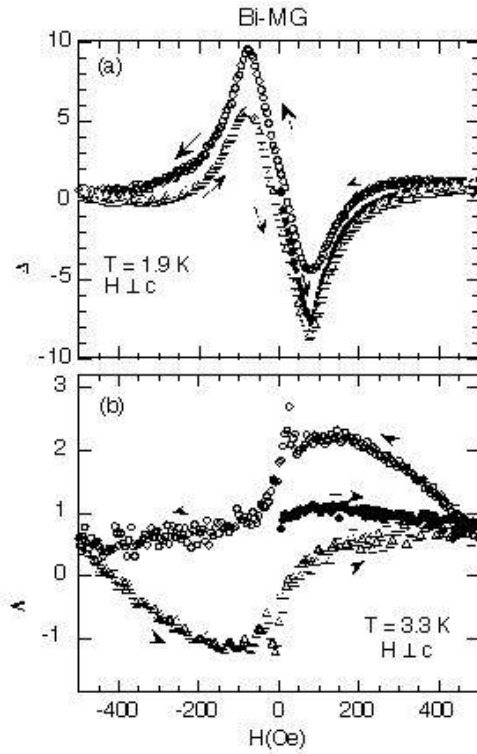


FIG. 4: Hysteresis loop of DC magnetization minus a diamagnetic background ($= \chi_d H$) for Bi-MG. $H \perp c$. (a) $T = 1.9$ K. $\chi_d = -5.143 \times 10^{-7}$ emu/gOe. (b) $T = 3.3$ K. $\chi_d = -7.317 \times 10^{-7}$ emu/gOe.

is defined by $M_c(H)$ at 1.9 K minus a diamagnetic background given by $\chi_d H$ with $\chi_d = -2.980 \times 10^{-6}$ emu/gOe. The hysteresis loop of M_c for $H \parallel c$ is very similar to the corresponding data M_a for $H \perp c$. The value of H_{c1} (≈ 75 Oe) for $H \parallel c$ is a little lower than that for $H \perp c$. The peak value of M_c is almost the same as that of M_a . The hysteresis loop of M_c at 1.9 K exhibits a nearly reversible behavior. In bulk samples this could be explained in terms of a lack of structural defects to provide pinning sites in the vortex state ($H_{c1} < H < H_{c2}$). In Bi-MG, however, the size of islands is much shorter than the coherence length. Thus the pinning effect is not relevant for these islands. In contrast, the hysteresis loop of M_a at 1.9 K exhibits some hysteretic behavior. Note that similar magnetization curves are observed in a superconductor TaC nanoparticles which are synthesized using a vapor-solid reaction path starting with carbon nanotube precursor.²⁴

B. Curie-like susceptibility due to nanographites

Figure 5 shows typical data of F_C for $H = 1$ kOe for $H \perp c$ and $H \parallel c$. The susceptibility is negative at high T and drastically increases with decreasing T . The least squares fit of the data (F_C vs T) for 1.9 $\leq T \leq 30$ K to

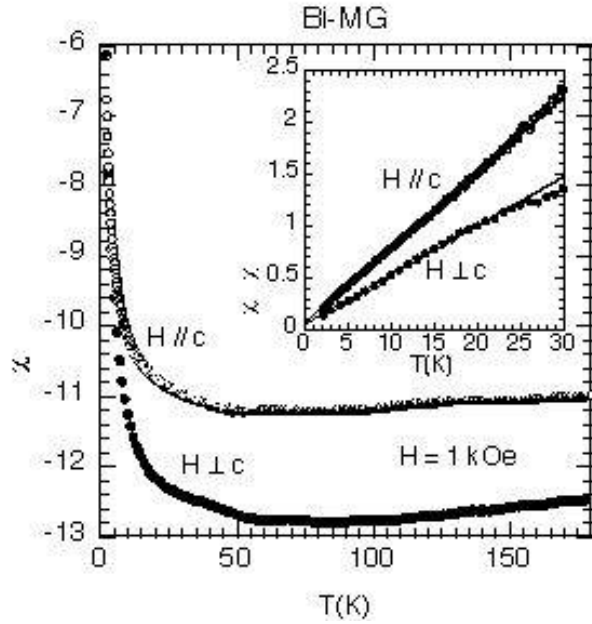


FIG. 5: T dependence of FC susceptibilities for Bi-MG. $H = 1$ kOe. $H \parallel c$ and $H \perp c$. The inset shows the reciprocal susceptibility $(\chi_0)^{-1}$ as a function of T . The solid lines are described by Eq.(2) with parameters given in the text.

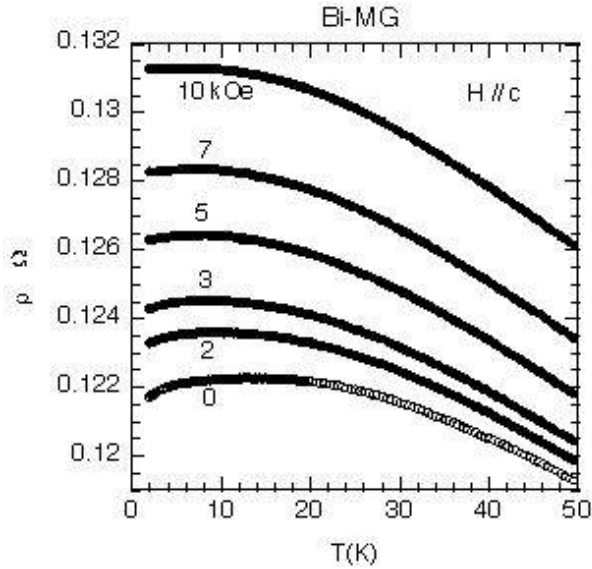


FIG. 6: T dependence of c-axis resistivity $\rho_c(T, H)$ for Bi-MG at various H . $H \parallel c$. 1 kH.

the Curie-Weiss law

$$\chi = \chi_0 + \frac{C}{T}; \quad (2)$$

yields $\chi_0 = -0.86 \pm 0.05$ K, $C = (1.999 \pm 0.029) \times 10^6$ emu K/g, $\chi_0 = (-1.307 \pm 0.001) \times 10^6$ emu/g for $H \parallel c$, and $\chi_0 = -1.13 \pm 0.02$ K, $C = (1.460 \pm 0.008) \times 10^6$ emu K/g, $\chi_0 = (-1.146 \pm 0.001) \times 10^6$ emu/g for $H \perp c$. The

value of χ_0 is very close to zero, showing a Curie-like law. In the inset of Fig. 5 we show the reciprocal susceptibility $(\chi_0)^{-1}$ as a function of T . The negative value χ_0 is from the orbital diamagnetic susceptibility. There is a crossover from the high-temperature diamagnetic susceptibility to the low-temperature Curie-like susceptibility around 50 K. We assume that the susceptibility of Bi-MG at 100 K corresponds to the diamagnetic susceptibility since the Pauli susceptibility is positive and is nearly equal to zero at 100 K. From Fig. 5 the diamagnetic susceptibility for $H \parallel c$ and $H \perp c$ is estimated as $\chi_c = -1.1 \times 10^6$ emu/g and $\chi_a = -1.3 \times 10^6$ emu/g, which are almost isotropic. These values are in contrast with the susceptibility of HOPG, which is very anisotropic: $\chi_c = -25.86 \times 10^6$ emu/g and $\chi_a = -1.06 \times 10^7$ emu/g at $H = 1$ kOe. The absolute value of χ_c in Bi-MG is much smaller than that in HOPG, while the values of χ_a are on the same order for both systems.

Here it is interesting to compare our data of susceptibility with that of nanographites prepared by heat treating diamond nanoparticles²⁵ and a disorder network of nanographites in activated carbon fiber (ACF).²⁶ The T dependence of the susceptibility for these compounds is similar to that of Bi-MG. In particular, the values of χ , C , and χ_0 for the ACF are on the same order as those for Bi-MG, where $\chi_0 = -2$ K, $C = 1.21 \times 10^6$ emu K/g, and $\chi_0 = -1.36 \times 10^6$ emu/g for ACF prepared at the heat treatment temperature $HTT = 1500$ °C.²⁶ Here we assume that the spin S is $1/2$ and the Lande g -factor is 2 since the spins are associated with carbon materials. The number of spin density per 1 g of Bi-MG is estimated as $(4.7 - 6.4) \times 10^{18}$ /g, which is comparable with 3.9×10^{18} /g for the ACF with $HTT = 1500$ °C.²⁶

It has been theoretically predicted by Wakabayashi et al.¹⁵ that the Pauli susceptibility exhibits a Curie-like behavior in the nanographites with zigzag edges, because of the DOS which is sharply peaked at the Fermi energy. However, qualitatively we think that the Curie-like behavior at low T in Bi-MG is due to the conduction electrons localized around the zigzag edges of nanographites, which have local magnetic moments (spin $S = 1/2$ and a Lande g -factor $g = 2$). The origin of spin polarization in nanographites with zigzag edges has been discussed by Fujita et al.¹³ using the Hamiltonian that consists of the on-site Coulomb repulsive interaction (U) when the site is occupied by two electrons, and the electron transfer integral between the nearest sites (t). They have shown that a ferrimagnetic spin polarization emerges on the edge carbons even for weak $U = t \approx 0.1$.

The orbital diamagnetic susceptibility is very sensitive to the size and edge shapes of nanographites. The orbital diamagnetic susceptibility is almost isotropic in Bi-MG, while it is very anisotropic in pristine graphite with infinite size. In Bi-MG the orbital cyclotron motion of electrons in the presence of H ($H \parallel c$) is greatly suppressed. This result is in good agreement with the prediction by Wakabayashi et al.¹⁵ In ribbon-shaped nanographites with zigzag edges, the magnitude of the diamagnetic sus-

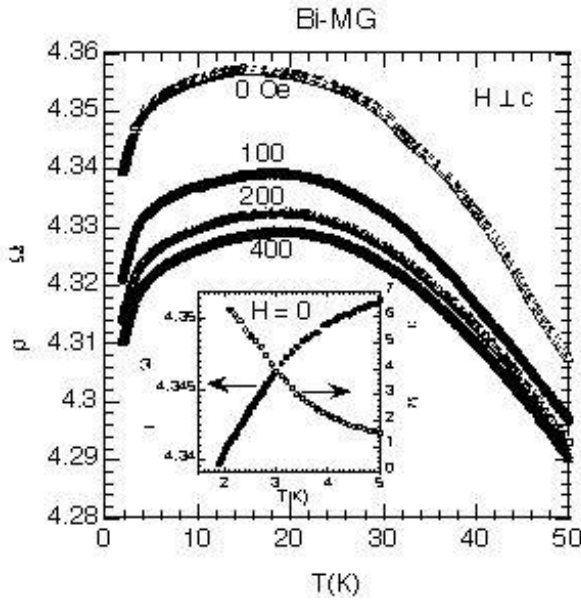


FIG. 7: T dependence of in-plane resistivity $\rho_a(T, H)$ for Bi-MG at $H = 0, 100, 200$, and 400 Oe. $H \parallel c$. The inset shows the T dependence of $\rho_a(T, H = 0)$ (—) and $d\rho_a(T, H = 0)/dT$ (---) at low T.

ceptibility decreases as the ribbon width decreases. The low of the orbital diamagnetic ring current significantly depends on the lattice topology near the graphite edge.

C. c-axis and in-plane resistivities

The c-axis resistivity ρ_c of Bi-MG was measured using the four-probe method. After the sample was cooled from 298 K to 1.9 K at $H = 0$, the c-axis resistivity ρ_c was measured with increasing T from 1.9 K to 50 K without and with H ($H \parallel c$ (c: c axis)), where the current direction is parallel to the field direction. This resistivity is denoted as the longitudinal magnetoresistance. Figure 6 shows the T dependence of ρ_c for Bi-MG at $H = 0 - 10$ kOe. The resistivity ρ_c for Bi-MG shows a very broad peak around 14 K at $H = 0$, in contrast to ρ_c for HOPG exhibiting a peak around 40 K.¹² This peak shifts to the low T side with increasing H . For $H = 20$ kOe, ρ_c shows a semiconductor-like behavior: it decreases with increasing T. Note that ρ_c shows a positive magnetoresistance: it increases with increasing H at any fixed T between 1.9 and 50 K. The value of ρ_c at $T = 298$ K and $H = 0$ is 0.11 cm , which is on the same order as that of HOPG ($\rho_c = 0.096 \text{ cm}$)¹² and BiCl₂BiCl₂ ($\rho_c = 0.2 \text{ cm}$),¹¹ leading to a mean free path less than 1 Å according to the Drude formula. This result suggests that there is no overlapping over nearest-neighbor layers along the c axis. The c-axis conduction can occur via the hopping of carriers between layers.

The in-plane resistivity ρ_a of Bi-MG was also measured using the four-probe method. After the sample

was cooled from 298 K to 1.9 K at $H = 0$, the in-plane resistivity ρ_a was measured with increasing T from 1.9 K to 50 K without and with H ($H \parallel c$), where the field direction is perpendicular to the current direction in the c plane. This resistivity is denoted as the transverse magnetoresistance. The resistivity ratio ($= \rho_c / \rho_a$) is estimated as 30 at 298 K using the measured ρ_a . However, the actual value of ρ_c is considered to be much larger than 30 because of possible contribution of ρ_c to the measured ρ_a . Figure 7 shows the T dependence of ρ_a of Bi-MG at $H = 0 - 400$ Oe. The zero-field ($H = 0$) in-plane resistivity increases with increasing T at low T, showing a metallic behavior. It has a maximum around 15 K, and it decreases with further increasing T, showing a semiconductor-like behavior. Note that the value of ρ_a for Bi-MG ($= 4.2 \text{ m cm}$) is much larger than that of BiCl₂BiCl₂ ($= 27 \text{ cm}$ at 298 K). We find that the T dependence of ρ_a for Bi-MG is very similar to that of grafoil: they even have similar magnitudes. The grafoil is a pyrolytic graphite with a polycrystalline structure formed of many domains. According to Koike et al.,²⁷ ρ_a of grafoil (grade GTA, Union Carbide) shows a semiconductor-like behavior, while ρ_a of HOPG (Union Carbide) shows a metallic behavior. This result suggests that the semiconductor-like behavior in Bi-MG may arise from nanographites where the degree of disorder is greatly enhanced. Such a semiconductor-like behavior is observed at least below 25 kOe.

In the inset of Fig. 7 we show the detail of ρ_a at $H = 0$ near $T_c = 2.48$ K. No drastic decrease in ρ_a below T_c is observed with decreasing T, while the T-derivative $d\rho_a/dT$ gradually decreases with increasing T around T_c . The causes for the finite value of ρ_a below T_c in spite of the superconducting phase are as follows. (i) The sample used in the present work is an exfoliated Bi-MG based on HOPG. The sample surface is not flat partly because of cracks generated in the basal plane. Since the current path is not always located on the same layer, the contribution of large ρ_c to the observed ρ_a is not negligibly small. Another possibility is the local superconductivity in isolated islands. In such a system there is competition between the Josephson coupling (E_J) and the charging energy (E_U) between superconducting islands.²⁸ For $E_J \gg E_U$, the Cooper pairs are delocalized leading to a superconducting state with vanishing resistivity. For $E_J \ll E_U$, the pairs will be localized and the transport is possible only by thermal activation leading to insulating behavior at $T = 0$ K. The resistivity varies with T as $\exp(T_a/T)$, where T_a is related to the activation energy. In this model, the resistivity should increase with decreasing T, which contradicts with our result. Liu et al.²⁹ have reported an unusual T dependence of resistivity at low H in ultrathin superconducting films of Pb, Al, and Bi. The resistivity varies with T as $\exp(T/T_0)$ at low T, where T_0 is a characteristic temperature. In Bi-MG, $d\rho_a/dT$ decreases with increasing T around T_c . In superconducting thin films, $d\rho_a/dT [\exp(T/T_0)/T_0]$ increases with increasing T. Therefore, the T dependence

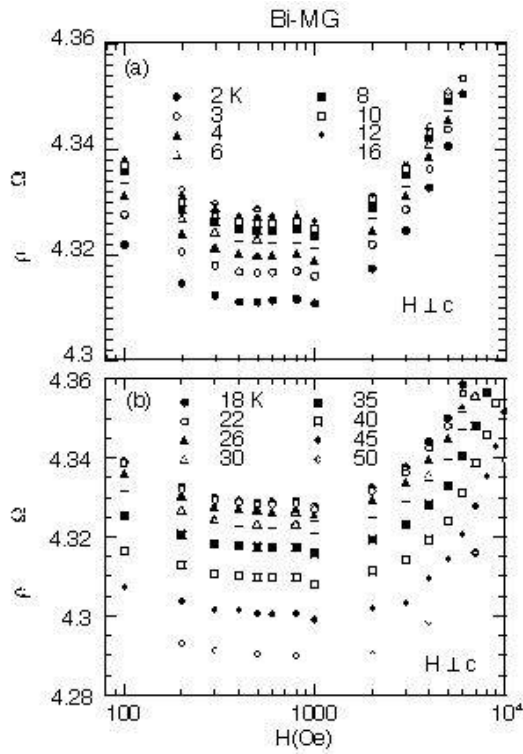


FIG. 8: H dependence of $\rho_a(T, H)$ for Bi-MG at fixed T (2 K \leq T \leq 50 K). $H \perp c$.

of ρ_a in Bi-MG is not the case of $\exp(T/T_0)$.

D. 2D Weak localization effect

As shown in Fig. 7, the in-plane resistivity ρ_a slightly decreases with increasing H at the same T (at least for 1.9 K \leq T \leq 50 K), indicating a negative magnetoresistance (NMR). Figures 8(a) and (b) show the H dependence of ρ_a for Bi-MG with 2 K \leq T \leq 50 K, where $H \perp c$ and the field direction is perpendicular to the current direction. For each T, ρ_a decreases with increasing H at low H ($H < 100$ Oe), exhibits a local minimum around $H = 2.5$ kOe, and increases with further increasing H. The sign of the difference $\Delta \rho_a = \rho_a(T; H) - \rho_a(T; H = 0)$ is negative for $0 < H < 3.5$ kOe due to the possible 2D weak localization effect (WLE).³⁰ It changes from negative to positive at $H = 3.5$ kOe. The resistivity ρ_a drastically increases with further increasing H, as is observed in compensated metals such as bulk Bi.³¹ The H dependence of ρ_a for 3 kOe $< H < 45$ kOe can be well described by $\rho_a = \rho_0 + \rho_1 H + \rho_2 H^2$, where ρ_0 , ρ_1 , and ρ_2 are constants: $\rho_0 = 4.290$ m Ω cm, $\rho_1 = (9.85 \pm 0.11) \times 10^3$ m Ω /Oe, and $\rho_2 = (4.56 \pm 0.23) \times 10^8$ m Ω /Oe² at 1.9 K. The linear term ($\rho_1 H$) is dominant compared to the squared-power term ($\rho_2 H^2$) for $H < H_1$, where $H_1 = \rho_1 / \rho_2 = 216$ kOe at 1.9 K. For comparison, we also measured the H dependence of ρ_a in Bi-MG for 1.9 K \leq T \leq 30 K, where $H \parallel c$. At each T, ρ_a increases with increasing H. Thus

the sign of ρ_a is always positive for $0 < H < 47.5$ kOe and 1.9 K \leq T \leq 50 K, indicating an anti-localization effect which is similar to that observed in Bi thin films³² with strong spin-orbit interactions.

The T dependence of ρ_a at $H = 45$ kOe for $H \perp c$ is described by

$$\rho_a = \rho_0 + \rho_1 \ln(T); \quad (3)$$

for 1.9 K \leq T \leq 4.3 K, where $\rho_0 = (4.8261 \pm 0.0002)$ m Ω cm and $\rho_1 = (3.79 \pm 0.19) \times 10^3$ m Ω cm. As shown in previous papers,^{12,33} the theory of the 2D WLE predicts that the following relation is valid for the ratio ρ_2/ρ_1 ,

$$\frac{\rho_2}{\rho_1} = \frac{e^2}{2\pi^2 h} \frac{A}{\rho_{2D}^0}; \quad (4)$$

with $A = p + 1$, where $e^2/(2\pi^2 h) = 1.23314 \times 10^5$ cm⁻¹ and ρ_{2D}^0 is the in-plane conductivity defined by I_c/ρ_a^0 (ρ_a^0 is the in-plane resistivity and I_c is the c axis repeat distance). In the parameter A, p is nearly equal to unity, p is the exponent of the inelastic lifetime of the conduction electrons ($\propto T^p$), and γ is a numerical factor giving a measure of the screening by other carriers. For convenience, here we use the value of $\rho_{2D}^0 = 1.89 \times 10^2$ cm⁻¹ for kish graphite ($I_c = 3.35$ A and $\rho_a^0 = 1.77$ cm at T = 4.2 K) obtained by Koike et al.,²⁷ instead of the corresponding data for Bi-MG. A kish graphite is a high-quality single crystal of graphite which is deposited on walls of blast furnaces for steel production. Using $\rho_1/\rho_2 = 7.853 \times 10^4$ the parameter A is estimated as $A = 1.20$, which is comparable with 1.14 for stage-4 MoC₁₈GIC.³³ These results suggest that the logarithmic behavior of ρ_a can be explained in terms of the 2D WLE.

E. Field induced metal-semiconductor transition

In Fig. 9(a) we show the T dependence of the difference ($\Delta \rho_a$) between ρ_a at T and that at 20 K for various H ($H \perp c$): $\Delta \rho_a = \rho_a(T; H) - \rho_a(T = 20 \text{ K}; H)$. The T dependence of $\Delta \rho_a$ below 10 K is dependent on H. The difference $\Delta \rho_a$ shows a metallic behavior ($d\rho_a/dT > 0$) below 15–20 kOe, while it shows a semiconductor-like behavior ($d\rho_a/dT < 0$) above $H = 25$ kOe. In Fig. 9(b) we show the T dependence of $\Delta \rho_a$ for $H \parallel c$. The T dependence of $\Delta \rho_a$ below 7 K is dependent on H. The difference $\Delta \rho_a$ shows a metallic behavior ($d\rho_a/dT > 0$) below 10 kOe, while it shows a semiconductor-like behavior above 20 kOe. Note that ρ_a at $H = 47.5$ kOe drastically increases with decreasing T, leading to the insulating state. The magnitude of $\Delta \rho_a$ for $H \parallel c$ is on the same order as that for $H \perp c$. The T dependence of $\Delta \rho_a$ at $H = 47.5$ kOe for $H \parallel c$ is well described by Eq.(3) for 1.9 K \leq T \leq 4.3 K, where $\rho_0 = (5.8385 \pm 0.0002)$ m Ω cm and $\rho_1 = (5.33 \pm 0.23) \times 10^3$ m Ω cm. The corresponding fitting curve is denoted by the solid line in the inset of Fig. 9(b). The ratio $\rho_1/\rho_2 = 9.13 \times 10^4$ is almost the same as that ($=$

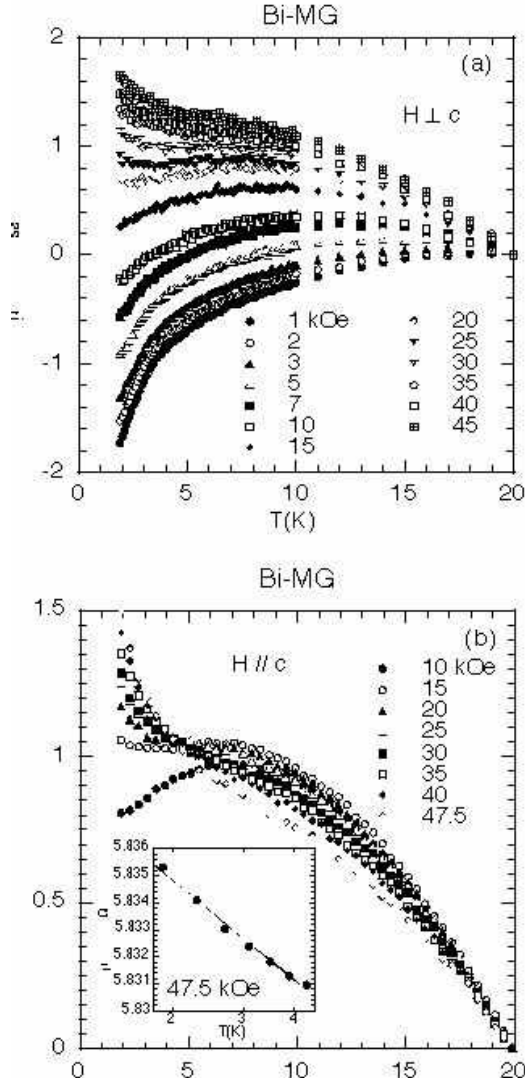


FIG. 9: T dependence of the difference Δa between $a(T; H)$ and $a(T = 20\text{K}; H)$ [$\Delta a = a(T; H) - a(T = 20\text{K}; H)$] for Bi-MG with various H (1 \leq H \leq 45 kOe). (a) $H \perp c$. (b) $H \parallel c$. The inset of (b) shows the T dependence of $\Delta a(T; H)$ at H = 47.5 kOe. The solid line denotes the fitting curve of the data to Eq.(3).

7.85 $\times 10^4$) for Δa at H = 45 kOe for $H \perp c$ (see Sec. IIIC), indicating the occurrence of 2D WLE.

Bi-MG undergoes a transition from the metallic phase to the semiconductor-like phase at a critical field H_c . Similar crossover behavior is observed in SiMOSEFET,³ and amorphous metal films of InO_x ,⁵ MoGe ,⁷ and Bi.⁸ The value of H_c (~ 25 kOe) for Bi-MG is almost the same as that for SiMOSEFET³ and amorphous MoGe film.⁷ Note that the Zeeman energy $g\mu_B H$ at 25 kOe corresponds to a thermal energy $k_B T_H$ with $T_H = 1.7$ K, where $g = 2$ and $S = 1/2$. The temperature T_H is slightly lower than T_c ($= 2.48$ K) for the superconductivity. The suppression of the metallic phase by H is independent of the directions of H ($H \parallel c$ and $H \perp c$) for Bi-MG. These results suggest that the spin related effect is significant compared to the orbital effect. This is consistent with the result derived from the susceptibility measurement that the Curie-like susceptibility is dominant at low T.

IV. CONCLUSION

Bi-MG shows superconductivity at $T_c = 2.48$ K, where the coherence length is much larger than the size of nanoparticles. The spin related effect characterized by a Curie-like susceptibility is enhanced, while the orbital effect is greatly suppressed. The transition from metallic phase to semiconductor-like phase is induced by the application of H above 25 kOe. A negative magnetoresistance in Δa and a logarithmic divergence of Δa with decreasing T are indicative of the 2D WLE.

Acknowledgments

We would like to thank Kikuo Harigaya for valuable comments on the magnetism of nanographites with zigzag edges. The work at SUNY-Binghamton was supported by SUNY-Research Foundation (Grant No. 240-9522A). The work at Osaka University was supported by the Ministry of Cultural Affairs, Education and Sport, Japan under the grant for young scientists (No. 70314375) and by Kansai Invention Center, Kyoto, Japan. We were grateful to Advanced Ceramics Corporation, Ohio for providing us with HOPG (grade ZYA).

suzuki@binghamton.edu

- ¹ E. Abraham, P. W. Anderson, D. C. Licciardello, and T. V. Ramakrishnan, Phys. Rev. Lett. 42, 673 (1979).
- ² S. V. Kravchenko, W. E. Mason, G. E. Bowker, J. E. Fumeaux, V. M. Pudalov and M. D'Orto, Phys. Rev. B 51, 7038 (1995).
- ³ D. Simonian, S. V. Kravchenko, M. P. Sarachik, and V. M. Pudalov, Phys. Rev. Lett. 79, 2304 (1997).
- ⁴ S. V. Kravchenko and T. M. Klapwijk, Phys. Rev. Lett. 84, 2909 (2000).

- ⁵ A. F. Hebard and M. A. Paalanen, Phys. Rev. Lett. 65, 927 (1990).
- ⁶ A. Li Yazdani and A. K. Apulnik, Phys. Rev. Lett. 74, 3037 (1995).
- ⁷ N. Mason and A. K. Apulnik, Phys. Rev. Lett. 82, 5341 (1999).
- ⁸ N. Markovic, C. Christiansen, and A. M. Goldman, Phys. Rev. Lett. 81, 5217 (1998).
- ⁹ J. Walter, H. Shioyama, and Y. Sawada, Carbon 36, 1811 (1998).

- ¹⁰ J. W alter and H .Shioyam a, Carbon 37, 1151 (1999).
- ¹¹ E .M cRae and J .W alter, Carbon 39, 717 (2001).
- ¹² M .Suzuki, C Lee, I.S.Suzuki, K .M atsubara, and K .Sugihara, Phys.Rev.B 54, 17128 (1996).
- ¹³ M .Fu jita, K .W akabayashi, K .N akada, and K .K usakabe, J.Phys.Soc.Jpn. 65, 1920 (1996).
- ¹⁴ K .W akabayashi, M .Sigrist, and M .Fu jita, J.Phys.Soc.Jpn. 67, 2089 (1998).
- ¹⁵ K .W akabayashi, M .Fu jita, H .A jiki, and M .Sigrist, Phys.Rev.B 59, 8271 (1999).
- ¹⁶ J.W alter and H .Shioyam a, Phys.Lett.A 254, 65 (1999).
- ¹⁷ J.W alter, Adv.M ater. 12, 31 (2000).
- ¹⁸ J.W alter, Phil.M ag.Lett. 80, 257 (2000).
- ¹⁹ D .B .H aviland, Y .Liu, and A M .G oldm an, Phys. Rev.Lett. 18, 2180 (1989).
- ²⁰ B .W eitzel and H .M icklitz, Phys. Rev. Lett. 66, 385 (1991).
- ²¹ G .D eutscher, O .Entin-W ohlm an, and Y .Shapira, Phys.Rev.B 22, 4264 (1980).
- ²² D .Saint-Jam es and P G .de G ennes, Phys. Lett. 7, 306 (1963).
- ²³ S.Tanum a, in G raphite Intercalation C om pounds II, edited by H .Zabel and S A .Soln (Springer-Verlag, Berlin, 1992) p.163.
- ²⁴ A .Fukunaga, S.Chu, and M .E .M cHenry, J.M ater.Res. 13, 2465 (1998).
- ²⁵ O .E .Andersson, B L.V .Prasad, H .Sato, T .Enoki, Y .H ishiyam a, Y .K aburagi, M .Yoshikawa, and S.Bandow, Phys.Rev.B 58, 16387 (1998).
- ²⁶ Y .Shibayam a, H .Sato, T .Enoki, and M .Endo, Phys.Rev.Lett. 84, 1744 (2000).
- ²⁷ Y .K oike, S.M orita, T .Nakam oto, and T .Fukase, J.Phys.Soc.Jpn. 54, 713 (1985).
- ²⁸ W .Zwenger, in Quantum Coherence in M esoscopic Systems, edited by B .Kramer (Plenum Press, New York, 1991) p.491.
- ²⁹ Y .Liu, D .B .H aviland, L.I.G lazman, and A M .G oldm an, Phys.Rev.Lett. 68, 2224 (1992).
- ³⁰ S .H ikam i, A .I. Larkin, and Y .Nagaoka, Prog. Theor. Phys. 63, 707 (1980).
- ³¹ M .Suzuki and S.Tanum a, J.Phys.Soc.Jpn. 45, 1645 (1978).
- ³² F .K om ori, S .K obayashi, and W .Sasaki, J.Phys.Soc.Jpn. 52, 368 (1983).
- ³³ M .Suzuki, I.S.Suzuki, K .M atsubara, and K .Sugihara, Phys.Rev.B 61, 5013 (2000).